Bargaining and Beamforming in Interference Channels

Rami Mochaourab and Eduard Jorswieck
Communications Theory, Communications Laboratory
Dresden University of Technology, Dresden, Germany
e-mail: {Rami.Mochaourab, Eduard.Jorswieck}@tu-dresden.de

Zuleita K. M. Ho and David Gesbert
EURECOM, 2229 route des crêtes
BP 193 F-06560 Sophia-Antipolis cedex
e-mail: {hokm, David.Gesbert}@eurecom.fr

***Abstract*—Utilizing the real-valued parametrization of each transmitter's efficient beamforming vectors, we propose a decentralized resource allocation scheme in the multiple-input single-output interference channel. The scheme is motivated by bargaining concepts in game theory. The aim of these concepts is to improve the joint payoff of the users from the Nash equilibrium outcome. In each bargaining-step, each user proposes a strategy. A user accepts any proposal if it increases his payoff. Otherwise, new proposals are made. When all proposals are accepted, a new bargaining-stage begins. We prove the scheme's convergence and demonstrate its performance by simulations. In comparison to previous approaches, our bargaining outcome is arbitrarily close to the Pareto boundary of the achievable single-user rate region. We further discuss the control overhead and complexity of this scheme.**

I. Introduction

We consider a setting in which two transmitter-receiver pairs utilize the same spectral band simultaneously. Each transmitter is equipped with N transmit antennas and each receiver with a single antenna. This setting corresponds to the multiple-input single-output (MISO) interference channel (IFC) [1]. The performance of the systems in such a setting is degraded by mutual interference, and their noncooperative operation is usually not efficient [2]. Therefore, coordination between the links is needed in order to improve the joint outcome. In game theory, bargaining describes the process in which the bargainers make use of an opportunity to gain by coordinating their actions [3]. In this work, we consider strategic bargaining between the links. The links decide on their actions at each bargaining-step and bargain as long as they experience improvement in their situation.

For the two-user MISO IFC, the efficient beamforming vectors of each transmitter are parameterized by a single real-valued parameter between zero and one in [4]. This parametrization is valuable for designing efficient low complexity distributed resource allocation schemes. In [5], this parametrization is utilized and a bargaining algorithm is proposed that requires two bit signaling between the transmitters. In each bargaining-step, the transmitters reduce their beamforming parameters by an equal step-length leading to a joint increase in the links' performance. In [6] a similar algorithm is proposed. At each bargaining-step, each transmitter optimizes its transmission to reduce a fixed amount of interference power at unintended receivers. Both algorithms in [5] and [6] terminate when at least one link experiences reduction in its outcome. While both algorithms improve the joint performance of the systems from the noncooperative state, these outcomes are however not Pareto optimal. In [7], a distributed algorithm is proposed that is performed between link pairs in a multi-link system. The transmitters exchange interference levels (scalar values) in each iteration and optimize their transmission such that the interference levels are met at unintended receivers. The interference levels are updated based on a necessary condition for Pareto optimality. Although this condition is not proven to be also sufficient, numerical evidence shows that the algorithm converges to a Pareto optimal outcome almost surely.

In this work, we propose a bargaining process between two links. The preference representation of the links in the Edgeworth box [8] is utilized in order to describe this process. We determine how each transmitter chooses its beamforming vectors in each bargaining-step such that the bargaining outcome lies arbitrarily close to the contract curve. The contract curve in the Edgeworth box corresponds to all Pareto optimal outcomes. Thus, our process is to converge to an outcome which is arbitrarily close to the Pareto boundary. Our algorithm requires four bit signaling between the transmitters in each bargaining-step, and we show that only a few iterations are necessary for the bargaining process to converge.

Notations: Column vectors and matrices are given in lowercase and uppercase boldface letters, respectively. $\|\boldsymbol{a}\|$ is the Euclidean norm of $\boldsymbol{a}, \boldsymbol{a} \in \mathbb{C}^N$. $|b|$ is the absolute value of $b, b \in \mathbb{C}$. $(\cdot)^H$ denotes the Hermitian transpose. The orthogonal projector onto the column space of $\boldsymbol{Z}$ is $\boldsymbol{\Pi}_Z := \boldsymbol{Z}(\boldsymbol{Z}^H\boldsymbol{Z})^{-1}\boldsymbol{Z}^H$. The orthogonal projector onto the orthogonal complement of the column space of $\boldsymbol{Z}$ is $\boldsymbol{\Pi}_Z^{\perp} := \boldsymbol{I} - \boldsymbol{\Pi}_Z$, where $\boldsymbol{I}$ is an identity matrix. Throughout the paper, the subscripts k, ℓ are from the set $\{1, 2\}$.

II. Preliminaries

A. System and Channel Model

The quasi-static block flat-fading channel vector from transmitter k to receiver ℓ is denoted by $\boldsymbol{h}_{k\ell} \in \mathbb{C}^N$. We assume

Part of this work has been performed in the framework of the European research project SAPHYRE, which is partly funded by the European Union under its FP7 ICT Objective 1.1 - The Network of the Future. This work is also supported in part by the Deutsche Forschungsgemeinschaft (DFG) under grant Jo 801/4-1.

that transmission consists of scalar coding followed by beamforming. The beamforming vector used by transmitter k, is $\boldsymbol{w}_k \in \mathbb{C}^N$. The matched-filtered, symbol-sampled complex baseband data received at the receivers is:

$$y_k = \boldsymbol{h}_{kk}^H \boldsymbol{w}_k s_k + \boldsymbol{h}_{\ell k}^H \boldsymbol{w}_\ell s_\ell + n_k, \quad k \neq \ell, \tag{1}$$

where s_k is the symbol transmitted by transmitter k. The random variables n_k are noise terms which we model as independent and identically distributed (i.i.d.) complex Gaussian with zero mean and variance σ^2. Each transmitter has a total power constraint of $P \triangleq 1$ such that $\|\boldsymbol{w}_k\|^2 \leq 1$.

Each transmitter is assumed to have perfect local channel state information (CSI), i.e., it has perfect knowledge of the channel vectors only between itself and all receivers. In addition, each receiver can measure the interference plus noise power and feedback this amount to its intended transmitter. We assume there exists a low bit rate communication link of high reliability between the transmitters. This enables signaling between the links during the bargaining process.

B. SINR Region and Efficient Transmission

The signal-to-interference-plus-noise ratio (SINR) at receiver k is

$$\phi_k(\boldsymbol{w}_1, \boldsymbol{w}_2) = |\boldsymbol{h}_{kk}^H \boldsymbol{w}_k|^2 / (|\boldsymbol{h}_{\ell k}^H \boldsymbol{w}_\ell|^2 + \sigma^2), \quad k \neq \ell. \tag{2}$$

This results in the achievable rate $\log_2(1+\phi_k(\boldsymbol{w}_1, \boldsymbol{w}_2))$ when the receivers perform single user decoding. The SINR region:

$$\Phi \triangleq \big\{(\phi_1(\boldsymbol{w}_1, \boldsymbol{w}_2), \phi_2(\boldsymbol{w}_1, \boldsymbol{w}_2)) : \|\boldsymbol{w}_k\|^2 \leq 1\big\}, \tag{3}$$

is the set of all SINR tuples achieved by feasible beamforming vectors. In the SINR region, tuples can be ranked by their Pareto efficiency. An operating point (Q_1, Q_2) is Pareto superior to an operating point (R_1, R_2) if $(Q_1, Q_2) \geq (R_1, R_2)$, where the inequality is componentwise and strict for at least one component. The transition from (R_1, R_2) to (Q_1, Q_2) is called a *Pareto improvement*. Situations where Pareto improvements are not possible are called *Pareto optimal*. These points constitute the Pareto boundary of the SINR region.

The beamforming vectors that are relevant for Pareto optimal operation in the MISO IFC are [4, Corollary 1]:

$$\boldsymbol{w}_k(\lambda_k) = \sqrt{\lambda_k} \frac{\boldsymbol{\Pi}_{\boldsymbol{h}_{k\ell}} \boldsymbol{h}_{kk}}{\|\boldsymbol{\Pi}_{\boldsymbol{h}_{k\ell}} \boldsymbol{h}_{kk}\|} + \sqrt{1-\lambda_k} \frac{\boldsymbol{\Pi}^{\perp}_{\boldsymbol{h}_{k\ell}} \boldsymbol{h}_{kk}}{\|\boldsymbol{\Pi}^{\perp}_{\boldsymbol{h}_{k\ell}} \boldsymbol{h}_{kk}\|}, \tag{4}$$

where $\lambda_k \in [0,1]$ and $k \neq \ell$. The set of beamforming vector in (4) includes maximum ratio transmission (MRT) ($\lambda_k^{\text{MRT}} = \|\Pi_{\boldsymbol{h}_{k\ell}} \boldsymbol{h}_{kk}\|^2 / \|\boldsymbol{h}_{kk}\|^2$) and zero forcing transmission (ZF) ($\lambda_k^{\text{ZF}} = 0$). According to [4, Corollary 2], it suffices that the parameters λ_k only be from the set $[\lambda_k^{\text{ZF}}, \lambda_k^{\text{MRT}}]$ for Pareto optimal operation. In the rest of the paper, we will write $\phi_k(\lambda_1, \lambda_2)$ instead of $\phi_k(\boldsymbol{w}_1(\lambda_1), \boldsymbol{w}_2(\lambda_2))$.

Lemma 1: $\phi_k(\lambda_1, \lambda_2)$ is monotonically increasing in λ_k, $\lambda_k \in [\lambda_k^{\text{ZF}}, \lambda_k^{\text{MRT}}]$ for fixed λ_ℓ, and monotonically decreasing in λ_ℓ for fixed λ_k, $k \neq \ell$.

Proof: The proof can be found in [9, Section IV.A]. ■

The monotonicity property of the SINRs is essential for the preference representation of the links discussed in the next section.

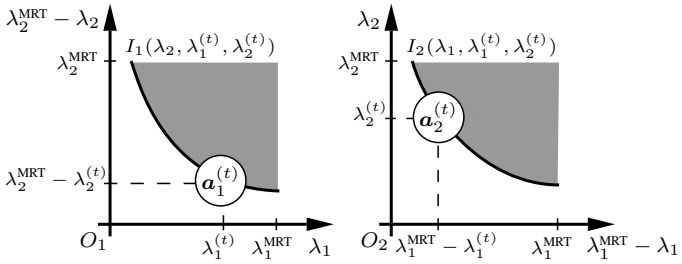

Fig. 1. Preference representation for each player.

III. Game Theoretic Analysis

A. Noncooperative Game

The links' noncooperative outcome is the solution of a strategic game [10, Section 2.1] between them. The set of players is $\{1, 2\}$ consisting of the two links. The pure strategies of player k are the real-valued parameters $\lambda_k \in [\lambda_k^{\text{ZF}}, \lambda_k^{\text{MRT}}]$ in (4), and his utility function is $\phi_k(\lambda_1, \lambda_2)$ in (2). In this game, a player always chooses the MRT strategy independent of the choice of the other player [2], i.e., MRT is a dominant strategy for each player. Hence, the unique Nash equilibrium (NE) is $(\lambda_1^{\text{MRT}}, \lambda_2^{\text{MRT}})$. The outcome in NE is usually not Pareto optimal. In order to achieve Pareto improvements from the NE, the players are required to cooperate. For this purpose, we assume there exists exogenous enforcement that compels the players to negotiate and apply any negotiated strategies.

B. Multi-stage Bargaining

Cooperation between the players is enabled by allowing them to communicate. In this way, they can exchange proposals as well as their preferences to the proposal outcomes. The act of proposal exchange based on the players' preferences can be modeled as a bargaining process. This process is sequential, and at each bargaining-step t, player 1 proposes $\lambda_1^{(t)}$ to player 2, and player 2 proposes $\lambda_2^{(t)}$ to player 1. In a general bargaining process, the players exchange amounts of goods within themselves. In our setting these goods will stand for the strategies of the players. According to Lemma 1, player 1 has higher payoff with a larger λ_1 and also a larger $\lambda_2^{\text{MRT}} - \lambda_2$. We define the *possession vector* of player 1 at a bargaining-step t as $\boldsymbol{a}_1^{(t)} = (\lambda_1^{(t)}, \lambda_2^{\text{MRT}} - \lambda_2^{(t)})$, where $\lambda_1^{(t)}$ is the amount of his good and $(\lambda_2^{\text{MRT}} - \lambda_2^{(t)})$ is the amount of good from player 2. Similarly, $\boldsymbol{a}_2^{(t)} = (\lambda_1^{\text{MRT}} - \lambda_1^{(t)}, \lambda_2^{(t)})$ is the possession vector of player 2. $\boldsymbol{a}_1^{(t)}$ and $\boldsymbol{a}_2^{(t)}$ are plotted in Fig. 1 (left) and (right), respectively, where the x-axis describes the good of player 1 and the y-axis that of player 2. In Fig. 1, I_k is the *indifference curve* of player k. This curve represents the pairs (λ_1, λ_2) such that $\phi_k(\lambda_1, \lambda_2) = \phi_k(\lambda_1^{(t)}, \lambda_2^{(t)})$. The dark region above I_k, represents the pairs (λ_1, λ_2) such that $\phi_k(\lambda_1, \lambda_2) > \phi_k(\lambda_1^{(t)}, \lambda_2^{(t)})$, and the region below I_k corresponds to less payoff for player k.

The bargaining process is structured in stages. A bargaining-stage, indexed with s, can span several bargaining-steps. In the first stage, $s = 0$, the possession vectors correspond to NE. i.e., $\boldsymbol{a}_1^{(s)} = (\lambda_1^{\text{MRT}}, 0)$ and $\boldsymbol{a}_2^{(s)} = (0, \lambda_2^{\text{MRT}})$. If at a

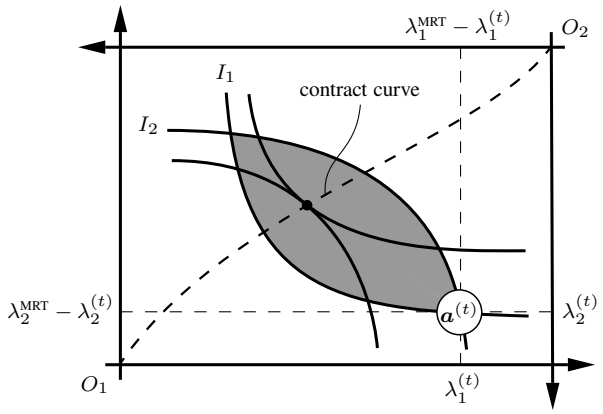

Fig. 2. An illustration of an Edgeworth box.

bargaining-step $t, t > s$, $(\phi_1(\lambda_1^{(t)}, \lambda_2^{(t)}), \phi_2(\lambda_1^{(t)}, \lambda_2^{(t)}))$ is a Pareto improvement to $(\phi_1(\lambda_1^{(s)}, \lambda_2^{(s)}), \phi_1(\lambda_1^{(s)}, \lambda_2^{(s)}))$ then we set $s = t$. This means that a new bargaining-stage begins each time a Pareto improvement is achieved. The players then compare their outcomes at each bargaining-step t to their current stage outcome (corresponding to bargaining-step s).

C. Edgeworth Box Representation

The Edgeworth box [8], [11, Chapter 5], illustrated in Fig. 2, is a graphical representation that is useful for the analysis of a bargaining situation. The box is constructed in joining Fig. 1 (left) and Fig. 1 (right) (rotated 180 degrees anticlockwise). Thus, the Edgeworth box has two points of origin, O_1 and O_2, corresponding to player 1 and 2, respectively. The initial amounts of goods of the players define the size of the box (width is λ_1^{MRT}, height is λ_2^{MRT}). The possession vectors $\boldsymbol{a}_1^{(t)}$ and $\boldsymbol{a}_2^{(t)}$ make up the *allocation* $\boldsymbol{a}^{(t)} = (\boldsymbol{a}_1^{(t)}, \boldsymbol{a}_2^{(t)})$. Every point in the box denotes an allocation, i.e., an assignment of a possession vector to each player.

Lemma 2: For a fixed strategy λ_ℓ, there exists a strategy $\lambda_k, k \neq \ell$, that achieves the payoff $\phi_k(\lambda_1^{(t)}, \lambda_2^{(t)})$ if $\phi_k(\lambda_1^{(t)}, \lambda_2^{(t)}) \in \mathcal{F}_k(\lambda_\ell)$, where

$$\mathcal{F}_1(\lambda_2) \triangleq [\phi_1(\lambda_1^{\text{ZF}}, \lambda_2), \phi_1(\lambda_1^{\text{MRT}}, \lambda_2)], \quad (5)$$

$$\mathcal{F}_2(\lambda_1) \triangleq [\phi_2(\lambda_1, \lambda_2^{\text{ZF}}), \phi_2(\lambda_1, \lambda_2^{\text{MRT}})]. \quad (6)$$

Proof: The proof is provided in [12]. ■

The players' preferences in the Edgeworth box can be revealed according to their indifference curves.

Proposition 1: The indifference curves of player 1 and 2 for given payoffs $\phi_k(\lambda_1^{(t)}, \lambda_2^{(t)}) \in \mathcal{F}_k(\lambda_\ell), k \neq \ell$, are

$$I_1(\lambda_2, \lambda_1^{(t)}, \lambda_2^{(t)}) = f(\lambda_1^{\text{MRT}}, \phi_1(\lambda_1^{(t)}, \lambda_2^{(t)})/\phi_1(\lambda_1^{\text{MRT}}, \lambda_2)), \quad (7)$$

$$I_2(\lambda_1, \lambda_1^{(t)}, \lambda_2^{(t)}) = f(\lambda_2^{\text{MRT}}, \phi_2(\lambda_1^{(t)}, \lambda_2^{(t)})/\phi_2(\lambda_1, \lambda_2^{\text{MRT}})), \quad (8)$$

respectively, where $f(a, b) = (\sqrt{ab} - \sqrt{(1-a)(1-b)})^2$.

Proof: The proof is provided in [12]. ■

Note in Proposition 1, that player k does not need to know $\lambda_\ell, \ell \neq k$, specifically to calculate $I_k(\lambda_\ell, \lambda_1^{(t)}, \lambda_2^{(t)})$, but requires only the interference plus noise levels at receiver k.

The dark region in Fig. 2 is called the *lens* and contains all allocations that are Pareto improvements to the outcome in $\boldsymbol{a}^{(t)}$. The locus of all Pareto optimal points in the Edgeworth box is called the *contract curve* [8]. On these points, the indifference curves are necessarily tangent.

Lemma 3: The indifference curve $I_k(\lambda_\ell, \lambda_1^{(t)}, \lambda_2^{(t)}), k \neq \ell$, for given payoff $\phi_k(\lambda_1^{(t)}, \lambda_2^{(t)})$ is concave in λ_ℓ.

Proof: The proof is provided in [12]. ■

The indifference curves in Fig. 2 are illustrated to be convex to the origin due to the axes transformation. The convexity property of the players' indifference curves implies that these can only be tangent at a single point. Thus, the condition that the indifference curves are tangent at an allocation $\boldsymbol{a}^{(t)}$ is a necessary and sufficient condition for $\boldsymbol{a}^{(t)}$ to be on the contract curve, i.e., $(\phi_1(\lambda_1^{(t)}, \lambda_2^{(t)}), \phi_2(\lambda_1^{(t)}, \lambda_2^{(t)}))$ is on the Pareto boundary of the SINR region.

IV. Decentralized Bargaining Process

This section describes how the players choose their proposals at each bargaining-step. At a bargaining-step t, player k knows his SINR $\phi_k(\lambda_1^{(t)}, \lambda_2^{(t)})$ as well as his SINR $\phi_k(\lambda_1^{(s)}, \lambda_2^{(s)})$ for the current stage. We define the following capabilities of each player:

- Player k keeps track of step-length $\delta_k^{(t)}$ at each bargaining-step t. The initial step-length is $\delta_k^{(0)}$.
- Player k can change the sign of $\delta_k^{(t)}$ and also reduce its length by multiplying it with $\theta_k \in (0, 1)$.
- Player k can choose three types of proposals:
  (I) $\lambda_k^{(t+1)} = \lambda_k^{(t)}$
  (II) $\lambda_k^{(t+1)} = \lambda_k^{(t)} - \delta_k^{(t+1)}$
  (III) $\lambda_k^{(t+1)} = I_k(\lambda_\ell^{(t)}, \lambda_1^{(s)}, \lambda_2^{(s)}), \quad \ell \neq k.$
  From Proposition 1, proposal type (III) gives player k the payoff $\phi_k(\lambda_1^{(s)}, \lambda_2^{(s)})$ when player ℓ chooses $\lambda_\ell^{(t)}$.
- Player k sets $\Gamma_\ell = \texttt{true}$ if player ℓ, $\ell \neq k$, chooses proposal type (III) at the current bargaining-step.

The choice of player 1's proposal (analogously player 2) is described in the flowchart in Fig. 3. In Fig. 4 six Edgeworth boxes are illustrated. In all boxes, the indifference curves correspond to the stage allocation $\boldsymbol{a}^{(s)}$. The marked regions in Fig. 4 resemble the regions where the allocations $\boldsymbol{a}^{(t)}, t > s$, are possible with respect to the indifference curves. Note that all regions in the Edgeworth box are covered in the cases in Fig. 4, hence all possible positions of $\boldsymbol{a}^{(t)}$ are treated. These cases will aid in the description of our bargaining process.

Each player k can signal to the counter player one of four signals: B_k, A_k, R_k, and N_k. In Fig. 3, Player 1 chooses the signaling to player 2 based on conditions D_1, D_2, and D_3 (analogously for player 2). Condition D_1 is true if the current step-length $\delta_1^{(t)}$ is below an accuracy measure ϵ. If player k signals B_k, then all players alter their initial step-length as $\delta_k^{(0)} = -\theta_k \delta_k^{(0)}$ and set $\delta_k^{(t+1)} = \delta_k^{(0)}$. The new proposals are of type (II). This adaptation is necessary since $\boldsymbol{a}^{(t)}$ can be in the opposite direction to the lens (proposals in the regions marked with a prime in Fig. 4 (E 4)-(E 6)). Changing the sign

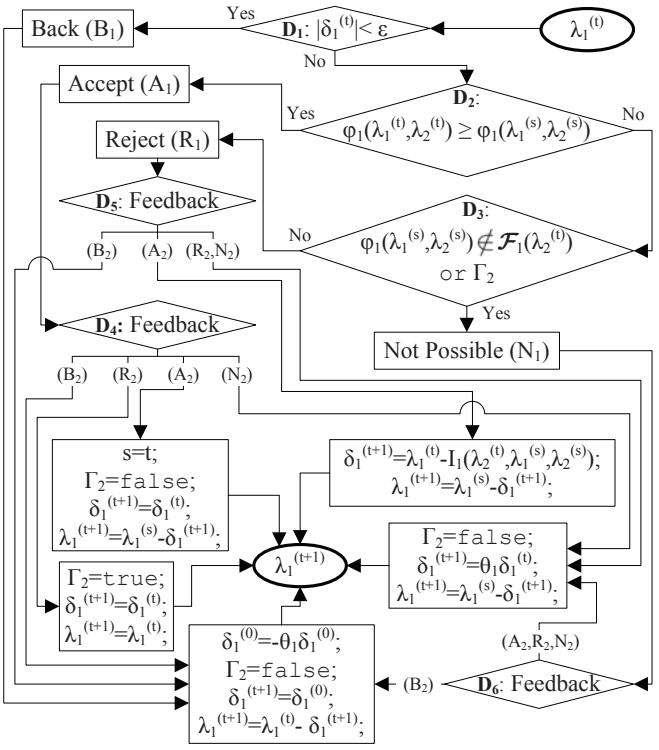

Fig. 3. Flowchart for player 1 (analogously player 2) for a new proposal.

of the step-length makes the allocations on the side of the lens. Since $\delta_1^{(t)}$ and $\delta_2^{(t)}$ always have the same sign, $\boldsymbol{a}^{(t)}$ will never be in the marked regions in Fig. 4 (E 1).

Condition D_2 is true if player 1 achieves an improvement in his payoff. Thus, player 1 accepts the proposal by signaling A_1 to player 2. If player 2 signals A_2, then the allocation $\boldsymbol{a}^{(t)}$ is necessarily in the lens in Fig. 4 (E 2), i.e., a Pareto improvement from the stage allocation is achieved. The new stage allocation is set as $\boldsymbol{a}^{(s)} = \boldsymbol{a}^{(t)}$ and both players choose proposal type (II) without altering the step-lengths. If player 2 signals R_2, then $\boldsymbol{a}^{(t)}$ is in region (a) in Fig. 4 (E 3). Player 2 chooses proposal type (III) and player 1 chooses proposal type (I). This adaptation is illustrated in Fig. 4 (E 3) as projecting the allocation $\boldsymbol{a}^{(t)}$ onto I_2. Player 1 sets $\Gamma_2 = \texttt{true}$. If player 2 signals N_2, then $\boldsymbol{a}^{(t)}$ is in region (a') in Fig. 4 (E 6) and above I_1. Both players then choose proposal type (II) which makes $\boldsymbol{a}^{(t+1)}$ closer than $\boldsymbol{a}^{(t)}$ to $\boldsymbol{a}^{(s)}$.

Condition D_3 is true if player 1 cannot find $\lambda_1^{(t+1)}$, given $\lambda_2^{(t)}$, to achieve $\phi_1(\lambda_1^{(s)}, \lambda_2^{(s)})$ as payoff (Lemma (2)). This case occurs if $\boldsymbol{a}^{(t)}$ is in the region marked in Fig. 4 (E 6), where $\boldsymbol{a}^{(t)}$ cannot be projected onto I_1 for constant $\lambda_2^{(t)}$. Condition D_3 is also true if Γ_2 is true, i.e., player 2 has chosen proposal type (III) in the previous step. This case reveals that the previous allocation $\boldsymbol{a}^{(t-1)}$ has been in any of the marked regions in Fig. 4 (E 4). Each player chooses proposal types (II) after reducing their step-lengths. Hence, $\boldsymbol{a}(t+1)$ will be closer to $\boldsymbol{a}(s)$. If D_3 is false, player 1 chooses his proposal according to the signaling from player 2. If player 2 signals (A_2), then this case is analogous to the case when player 1

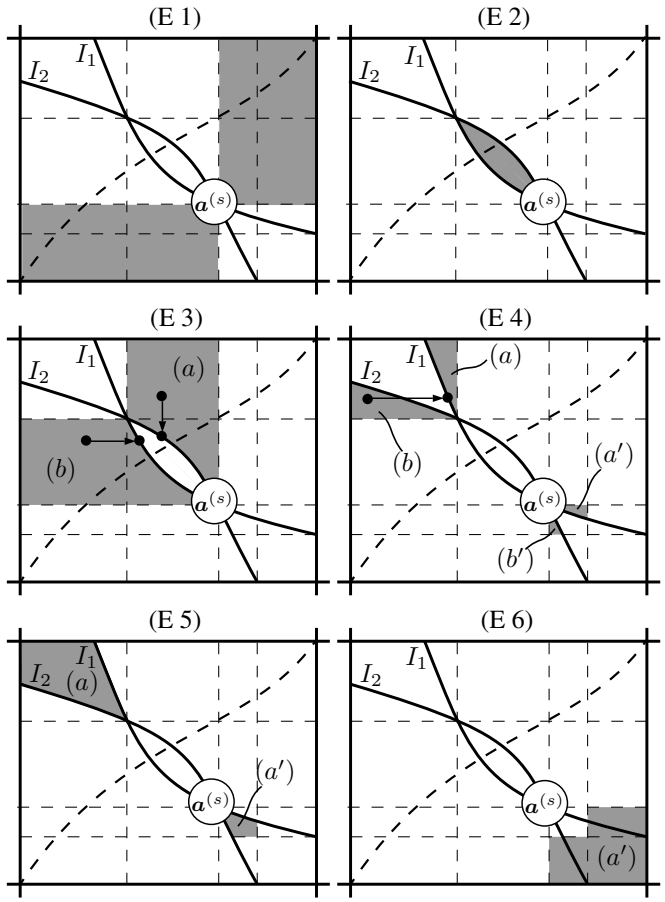

Fig. 4. Six Edgeworth boxes which illustrate the possible positions of the allocation $\boldsymbol{a}^{(t)}$ of a bargaining-step.

signals A_1 and player 2 R_2. If player 2 signals (R_2), then $\boldsymbol{a}^{(t)}$ can only be in regions (a) or (a') in Fig. 4 (E 5). Both players use proposal types (II) after reducing their step-lengths.

Convergence and Pareto Optimality: The bargaining process terminates when $|\delta_1^{(0)}| < \epsilon$ or $|\delta_2^{(0)}| < \epsilon$. The initial step-length $\delta_k^{(0)}$ is reduced each time B_k is signaled, i.e., when $|\delta_k^{(t)}| < \epsilon$. The step-length of at least one player is reduced in each bargaining-step, except when Pareto improvements are achieved. Pareto improvements lead to a reduction in the size of the lens. The lens vanishes when the indifference curves are tangent, i.e., the allocation is on the contract curve. Therefore, the bargaining process converges after a finite number of steps to an outcome arbitrarily close to the Pareto boundary.

V. Simulations

In Fig. 5, an SINR region for a sample channel realization is plotted using the set of efficient beamforming vectors in (4) (100 samples are taken uniformly in $[\lambda_k^{\text{ZF}}, \lambda_k^{\text{MRT}}]$). The upper right boundary of this region is the Pareto boundary. The ZF and NE outcomes correspond to $(\lambda_1^{\text{ZF}}, \lambda_2^{\text{ZF}})$ and $(\lambda_1^{\text{MRT}}, \lambda_2^{\text{MRT}})$, respectively. Three different outcomes achieved by our bargaining process are marked with squares. The bargaining trajectories from the NE to these outcomes corresponds to the

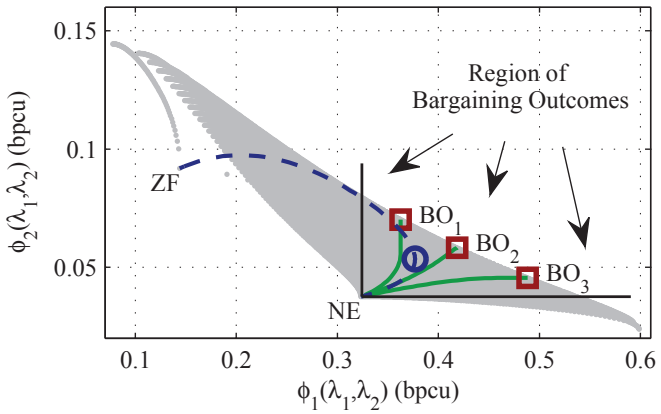

Fig. 5. SINR region of a two-user MISO IFC with signal-to-noise ratio (SNR) = 0 dB and two antennas at the transmitters. The bargaining outcomes are marked with squares for three different initial step-lengths $(\delta_1^{(0)}, \delta_2^{(0)})$. $BO_1 : (0.02, 0.01)$, $BO_2 : (0.015, 0.01)$, $BO_3 : (0.01, 0.01)$.

stages during the bargaining process. The bargaining outcome cannot be determined prior to the bargaining process and depends on the initializing parameters. However, this outcome always dominates the NE, e.g. BO_1, BO_2, and BO_3. The dashed line connecting NE and ZF is the trajectory curve of the bargaining algorithm proposed in [5]. In this algorithm both players start at the NE (or ZF) and reduce their proposals in equal step-lengths. The algorithm terminates when at least one player experiences reduction in his payoff. The outcome of this algorithm starting in NE is marked with a circle.

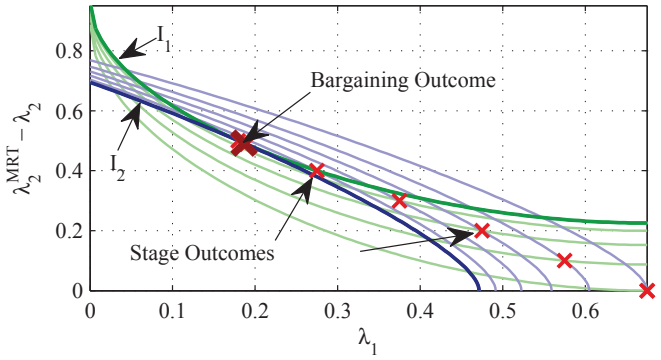

Fig. 6. Edgeworth box representation of the bargaining process for $(\delta_1^{(0)}, \delta_2^{(0)}) = (0.1, 0.1)$, $N = 2$, and SNR = 0 dB.

In Fig. 6, an Edgeworth box is plotted for the bargaining process in which $(\delta_1^0, \delta_2^0) = (0.1, 0.1)$ and $\epsilon = 10^{-5}$. The stage allocations are marked with crosses, and the lens is bounded by the corresponding indifference curves. The lens reduces in size after each bargaining-stage until the indifference curves are tangent at the bargaining outcome. This indicates that the outcome is Pareto optimal. In Fig. 7, the SINR values for the same setting as of Fig. 6 are plotted over the bargaining-steps. The stage outcomes are marked with circles. These are the SINR pairs that both players agreed on during the bargaining process. The algorithm terminates after 40 bargaining-steps. However, since the SINRs only increase slightly after half the

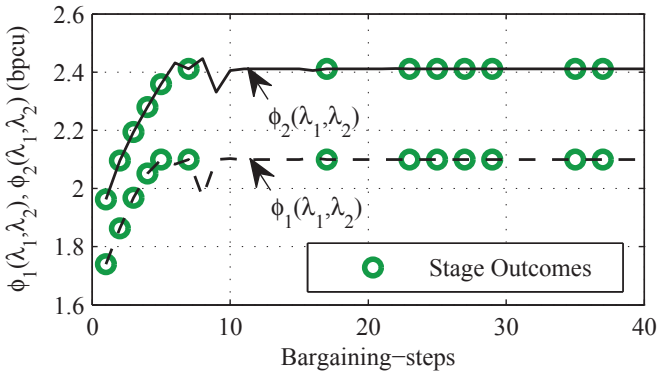

Fig. 7. SINR values over the bargaining-steps for $(\delta_1^{(0)}, \delta_2^{(0)}) = (0.1, 0.1)$, $N = 2$, and SNR = 0 dB.

bargaining-steps, the bargaining process could be stopped at bargaining-step 20 requiring a total of 80 signaling bits.

VI. Conclusions

In this work, we consider bargaining between two links in the MISO IFC. We propose a strategic bargaining process in which the links adapt their transmission based on the current bargaining situation. The adaptation is motivated by the Edgeworth box preference representation of the links. We prove the convergence of the bargaining process to an outcome which is arbitrarily close to the Pareto boundary and dominates the Nash equilibrium in the SINR region. Simulation results show that only few bargaining-steps are required for the bargaining process to converge. In each bargaining-step, four bit signaling between the links are required.

References

[1] S. Vishwanath and S. Jafar, "On the capacity of vector Gaussian interference channels," in *Proc. of ITW*, Oct. 2004, pp. 365–369.

[2] E. G. Larsson and E. A. Jorswieck, "Competition versus cooperation on the MISO interference channel," *IEEE J. Sel. Areas Commun.*, vol. 26, no. 7, pp. 1059–1069, Sept. 2008.

[3] J. C. Harsanyi, "Approaches to the bargaining problem before and after the theory of games: A critical discussion of Zeuthen's, Hicks', and Nash's theories," *Econometrica*, vol. 24, no. 2, pp. 144–157, 1956.

[4] E. A. Jorswieck, E. G. Larsson, and D. Danev, "Complete characterization of the Pareto boundary for the MISO interference channel," *IEEE Trans. Signal Process.*, vol. 56, no. 10, pp. 5292–5296, Oct. 2008.

[5] Z. K. M. Ho and D. Gesbert, "Spectrum sharing in multiple-antenna channels: A distributed cooperative game theoretic approach," in *Proc. of PIMRC*, Sept. 2008, pp. 1–5.

[6] J. Lindblom and E. Karipidis, "Cooperative beamforming for the MISO interference channel," in *Proc. of 16th European Wireless Conference (EW'10)*, 2010.

[7] R. Zhang and S. Cui, "Cooperative interference management with MISO beamforming," *IEEE Trans. Signal Process.*, vol. 58, no. 10, pp. 5454–5462, Oct. 2010.

[8] F. Y. Edgeworth, *Mathematical Psychics: An Essay on the Application of Mathematics to the Moral Sciences*. London, U.K.: C. K. Paul, 1881.

[9] E. A. Jorswieck and E. G. Larsson, "Monotonic optimization framework for the two-user MISO interference channel," *IEEE Trans. Commun.*, vol. 58, pp. 2159–2168, July 2010.

[10] M. J. Osborne and A. Rubinstein, *A Course in Game Theory*. The MIT Press, 1994.

[11] G. A. Jehle and P. J. Reny, *Advanced Microeconomic Theory*, 2nd ed., ser. Addison-Wesley. Pearson Education, 2003.

[12] R. Mochaourab, E. A. Jorswieck, K. M. Z. Ho, and D. Gesbert, "Bargaining and beamforming in interference channels," in preparation.